

Synthesis, characterization and complexation of Schiff base ligand *p*-anisalcefuroxime with Cu²⁺ and Fe²⁺ ions; antimicrobial and docking analysis with PBP2xto study pharmacokinetic parameters

Farhana Hoque^{1†}  , Nazmun Nahar¹  , Fahmida S. Annie¹  , Afsana Rahim¹  
Mohammed K. Hossain²  , Mohammad N. Abdul Rahman³  , Khaled A. A. Alkadi³  
Rosidah B. Shardin³, Nor Akmalayati Sulong³, and Abul Kalam Azad^{3*†}  

¹ Department of Pharmacy, Faculty of Basic Medical and Pharmaceutical Sciences, University of Science and Technology Chittagong, Chattogram, Bangladesh

² Department of Pharmacy, Faculty of Biological Sciences, University of Chittagong, Chattogram, Bangladesh

³ Department of Pharmaceutical Technology, Faculty of Pharmacy, University College MAIWP International, 68100 Kuala Lumpur, Malaysia

* Author to whom correspondence should be addressed, † Authors are equally contributed

Article number: 185, Received: 02-12-2024, Accepted: 12-01-2025, Published online: 17-01-2025

Copyright© 2025. This open-access article is distributed under the *Creative Commons Attribution License*, which permits unrestricted use, distribution, and reproduction in any medium, provided the original work is properly cited.

HOW TO CITE THIS

Hoque et al. (2025) Synthesis, characterization and complexation of Schiff base ligand *p*-anisalcefuroxime with Cu²⁺ and Fe²⁺ ions; antimicrobial and docking analysis with PBP2xto study pharmacokinetic parameters.

Mediterr J Pharm Pharm Sci. 5 (1): 48-64. [Article number: 185]. <https://doi.org/10.5281/zenodo.14647651>

Keywords: Antibacterial, cefuroxime, metal complexes, molecular docking, *p*-anisaldehyde, PBP2x

Abstract: Schiff base ligands and their metal complexes are considered promising leads in the development of new drugs. Due to their outstanding ability to form chelate complexes, they readily interact with transition metals that possess vacant orbitals. Several benefits are associated with transition metal complexes due to their favorable biocompatibility and low toxicity in biological systems. This study seeks to investigate the synthesis of a novel Schiff base derived from two starting materials: *p*-anisaldehyde and cefuroxime. The *p*-anisalcefuroxime complex was synthesized by coordinating it with metal ions of Cu²⁺ and Fe²⁺, resulting in the formation of new metal complexes. The antibacterial properties of these compounds were examined against gram-positive and gram-negative bacterial strains. These synthesized compounds were characterized using infrared spectroscopy (IR), nuclear magnetic resonance (NMR) spectroscopy ¹H NMR, ¹³C NMR and UV spectral data, along with melting point measurement, chemical testing, thin-layer chromatography (TLC) analysis, colour testing, and solubility assessments, *etc.* Molecular docking analysis was concluded by docking SB ligands with PBP2x of *Streptococcus pneumoniae*, revealing the binding affinity of the SB ligand. The pharmacokinetic parameters of the SB ligand were studied using online web tools such as Swiss absorption, distribution, metabolism, and excretion (ADME), pkCSM, and admetSAR. Thus, the synthesized Schiff base ligand and its metal complexes exhibit significant antibacterial activity and promising pharmacokinetic properties, making them strong candidates for further development as antibacterial agents.

Introduction

Infectious diseases caused by bacteria have become a significant global health challenge, primarily due to the rapid development of antimicrobial resistance to existing drugs. One of the major contributors to this issue is the emergence of multidrug-resistant bacterial strains, including those resistant to common antibiotics like

cefuroxime. Cefuroxime, a second-generation cephalosporin, is a β -lactam antibiotic that targets bacterial cell wall synthesis by inhibiting peptidoglycan transpeptidation [1]. It is effective against both aerobic gram-positive microorganisms such as *Staphylococcus aureus* (*S. aureus*), *Streptococcus pneumoniae* (*S. pneumoniae*), *Streptococcus pyogenes* (*S. pyogenes*) and aerobic gram-negative microorganisms such as *Escherichia coli* (*E. coli*), *Haemophilus influenzae* (*H. influenzae*) including beta-lactamase-producing strains, *Haemophilus parainfluenzae* (*H. parainfluenzae*), *Klebsiella pneumoniae* (*K. pneumoniae*), *Moraxella catarrhalis* (*M. catarrhalis*) including beta-lactamase-producing strains, *Neisseria gonorrhoeae* (*N. gonorrhoeae*) including beta-lactamase-producing strains [2]. However, the rise of resistance, particularly against β -lactam antibiotics, poses a significant threat to its effectiveness. Resistance mechanisms such as β -lactamase production and alterations in penicillin-binding proteins (PBPs) have reduced cefuroxime's efficacy, especially against methicillin-resistant *S. aureus* (MRSA) strains that produce the *mecA* gene, encoding the PBP2a enzyme [3]. To combat the growing resistance problem, there has been increased interest in developing new antimicrobial compounds, including those based on metal complexes. Schiff bases (SB), which are compounds formed by the condensation of primary amines with carbonyl compounds, have demonstrated promising antimicrobial activities [4]. SB ligands derived from cephalosporins have attracted attention for their potential to enhance the antimicrobial properties of the parent antibiotic by coordinating with transition metal ions. Transition metals such as iron (Fe), copper (Cu), and zinc (Zn) are known to play crucial roles in bacterial enzymatic processes, and their complexes with SBs may enhance the antibacterial efficacy of these compounds [5].

Schiff bases derived from various aldehydes and amines have been reported to possess significant antibacterial properties. For example, SBs synthesized from salicylaldehyde and 2-hydroxyaniline have shown activity against *Mycobacterium tuberculosis* (*M. tuberculosis*) H37Rv, while those derived from isatin have exhibited antimicrobial activity against a variety of bacteria, including *E. coli* and *Vibrio cholera* (*V. cholera*) [4]. Moreover, SB metal complexes, such as those involving Fe and Cu, have demonstrated enhanced activity against gram-positive and gram-negative bacteria. These complexes can exert their antibacterial effects through mechanisms such as interference with bacterial respiration or the inhibition of key enzymes involved in bacterial growth [6]. The incorporation of metal ions into SB compounds may not only enhance their stability and solubility but also potentially overcome bacterial resistance mechanisms. For instance, Fe and Cu play pivotal roles in bacterial metabolism and can affect the activity of enzymes like urease, which is essential for bacterial growth [5]. Furthermore, SB metal complexes have been shown to interact with bacterial enzymes involved in cell wall synthesis and other essential functions, improving the bioactivity of these compounds. In the context of cefuroxime, SB ligands derived from p-anisaldehyde and cefuroxime have been synthesized, and their antimicrobial activities have been evaluated. These SB ligands, when complexed with Fe (II) and Cu (II), demonstrated improved antimicrobial properties compared to the parent antibiotic alone.

Recent antibacterial studies revealed that some of the synthesized derivatives exhibited effectiveness against tested microorganisms compared to the well-established antibacterial drug like ciprofloxacin. Furthermore, molecular interaction studies revealed that the synthesized molecules have a significant binding affinity toward human estrogen receptor alpha and CDK2/cyclin A proteins using molecular docking simulation [7]. Therefore, this study applied the same approach to identify the binding affinity and others. The synthesis of these complexes was characterized using various techniques, including IR, NMR (^1H and ^{13}C), UV spectroscopy, and melting point determination, which confirmed the formation of stable metal-ligand complexes. The antibacterial activity of these compounds was tested against common bacterial pathogens such as *S. aureus* and *S. pneumoniae*. Additionally, molecular docking studies were employed to evaluate the binding affinity of the SB ligands with PBP2x, a critical enzyme in bacterial cell wall synthesis. These findings suggested that the SB-metal complexes might inhibit bacterial growth by disrupting the function of PBPs.

Thus, the development of SB metal complexes derived from cefuroxime shows significant promise as a strategy to combat antibiotic resistance. The enhanced antimicrobial activity of these complexes, combined with their ability to target bacterial enzymes, offers a potential avenue for addressing the global issue of multi-drug resistance. This study seeks to investigate the synthesis of a novel SB derived from two starting materials: *p*-anisaldehyde and cefuroxime

Materials and methods

Reagent and chemicals: Cefuroxime, *p*-anisaldehyde, methanol, ethanol, HCl, *N*-hexane acetone, β -naphthol solution were obtained from Sigma-Aldrich (Sigma-Aldrich, 3050 Spruce St., Saint Louis, MO, United States, 63103), sodium nitrate solution, chloroform, $\text{FeSO}_4 \cdot 7\text{H}_2\text{O}$, $\text{CuSO}_4 \cdot 5\text{H}_2\text{O}$ were obtained from Labtex Bangladesh Ltd. (Bangladesh). All reagents used were of analytical grades.

Preparation of Schiff base ligand *p*-anisalcefuroxime: New SB (*p*-anisalcefuroxime) was prepared via the condensation of *p*-anisaldehyde with cefuroxime in a methanol solution. The mixture was refluxed at 80°C for 10 hrs with constant stirring by magnetic stirrer. The mixture was then cooled in ice-bath and kept overnight when orange-yellowish precipitate separated out. This was filtered off, washed with methanol and kept in desiccator. This was recrystallized by using methanol and purity of the ligand checked by TLC [8].

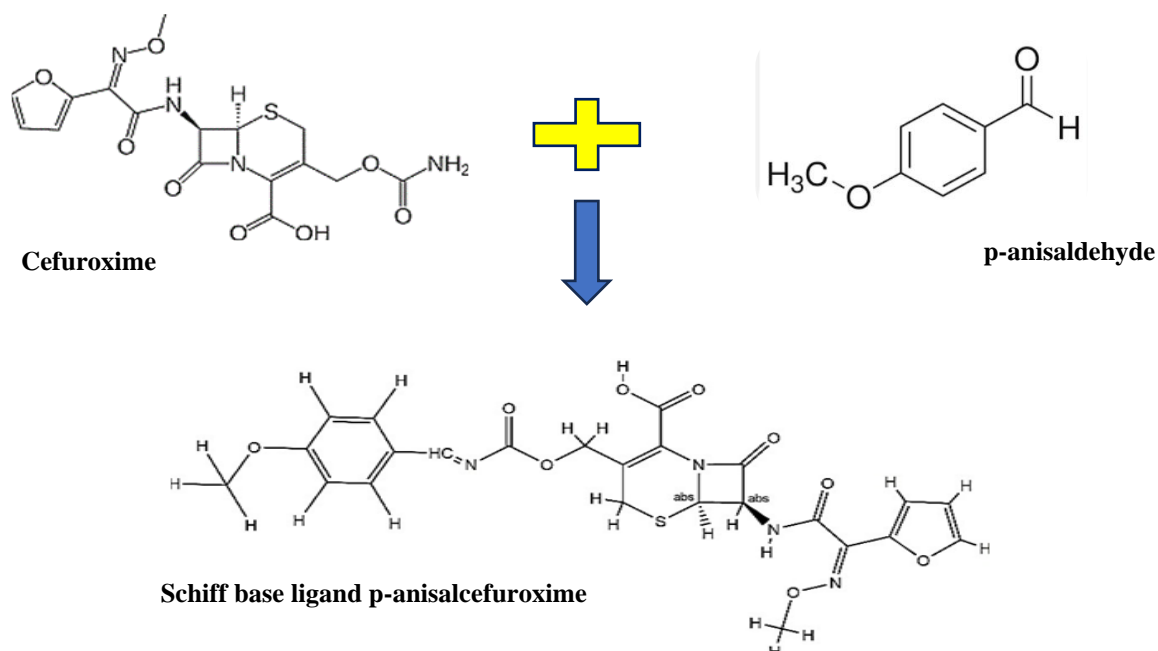


Figure 1: Preparation of *p*-anisaldehyde

Melting point measurements: An electro-thermal melting point apparatus was used for the determination of melting or decomposition points of the prepared ligands.

TLC and R_f value measurements

***p*-Anisaldehyde:** The TLC and R_f value of SB ligands were measured by using the solvent (10: 4), *n*-hexane: CHCl_3 . The instrument with UV light was used for the determination of TLC and R_f value of the prepared ligands.

***p*-Anisaldehyde and metal complexes:** The TLC was performed on Si gel pre-coated plates (PF254, 20×20 , 0.25 mm, Merck, Germany), and R_f value of Cu^{2+} were measured by using the solvent (10: 4) *n*-hexane: CHCl_3 .

Electronic spectra: Electronic spectra were run on a Shimadzu UV-visible 240 spectrophotometer. JASCO DIP-360 Digital polarimeter was used to measure the optical rotations in chloroform by using 10 cm cell tube.

¹H and ¹³C NMR ¹H and ¹³C NMR spectra were recorded on a Bruker Avance III 600 Ascend spectrometer using BBO probe operating at 125 MHz using CDCl₃ as solvent. Chemical shifts were reported in δ (ppm) and coupling constants (J) were measured in Hz.

Infrared spectra: Infrared spectra were recorded with Shimadzu (model-200-91527) and Shimadzu (model-4300) infrared spectrometers in the range 500-4000 cm⁻¹ [9].

Antibacterial assay: The antibacterial activities of the test complexes were studied against 10 human pathogenic bacteria. For the detection of antibacterial activities, the disc diffusion method was followed. Nutrient agar (NA) was used as basal medium for culture of test bacteria and methanol and water was used as a solvent to prepare the desired solution (2.0%) of the compounds initially. Proper control was maintained with solvent. The materials and methods of the present research work are described below in details [10].

Preparation of stock culture: Slants of NA for bacteria were prepared. 24 hrs old cultures were transferred to the fresh test tube slants separately with the help of sterilized wire loop. A number of test tube slant were freshly prepared for each bacterial pathogen. The inoculated slants were incubated at 35.0±2.0°C in an incubator. Bacterial suspensions were used to pour on the plate during sensitivity test. In this case, inoculum concentration was determined through gradual dilution technique. The diameters of zone of inhibition (in mm) of the standard drug cefuroxime was determined against *E. coli* and *S. aureus* [11].

Molecular docking analysis: The three-dimensional crystal structure of PBP2x from a highly penicillin-resistant *S. pneumoniae* (clinical isolate: a mosaic framework containing 83 mutations) was retrieved in pdb format from the protein data bank. For docking analysis, Autodock Vina was employed and AutoDock Tools (ADT) of the multi-platform graphics library (MGL) software package was used to convert pdb into a pdbqt format to input protein and ligands. The size of grid box in AutoDockVina was kept at size_x = 144.150229568, size_y = 152.005503521, size_z = 73.402777574. Autodock Vina was implemented through the shell script provided by AutoDock Vina developers. The binding affinity of ligand was observed by kcal/mole as a unit for a negative score.

Pharmacokinetic parameters study: For ADMET analysis, three most popular online web tools SwissADME, pkCSM and admetSAR that gives free access to a pool of fast yet robust predictive models for physicochemical properties, pharmacokinetics, drug-likeness and medicinal chemistry friendliness, among which in-house proficient methods such as the BOILED-Egg, iLOGP and Bioavailability Radar [12].

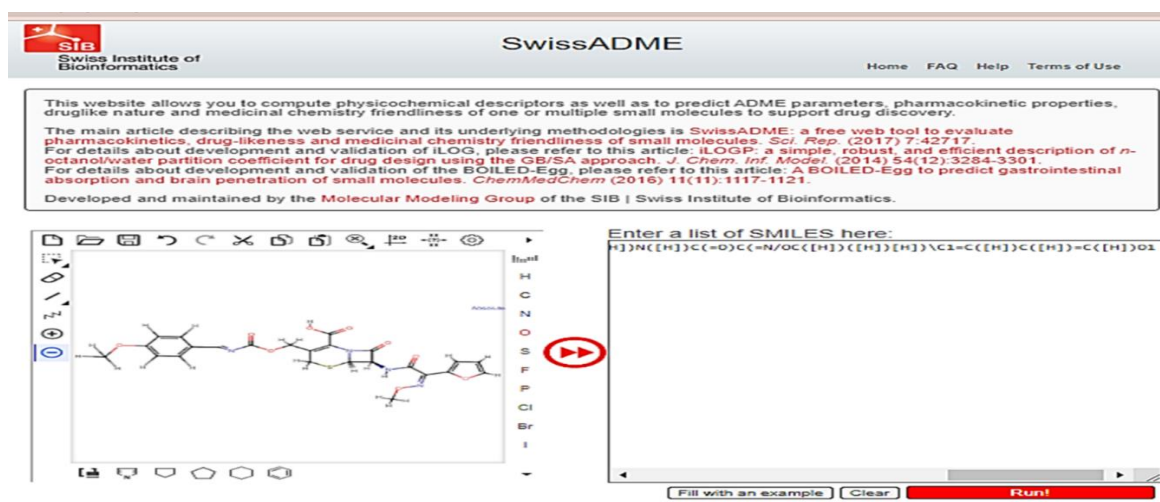


Figure 2: Web tools SwissADME, pkCSM, and admetSAR

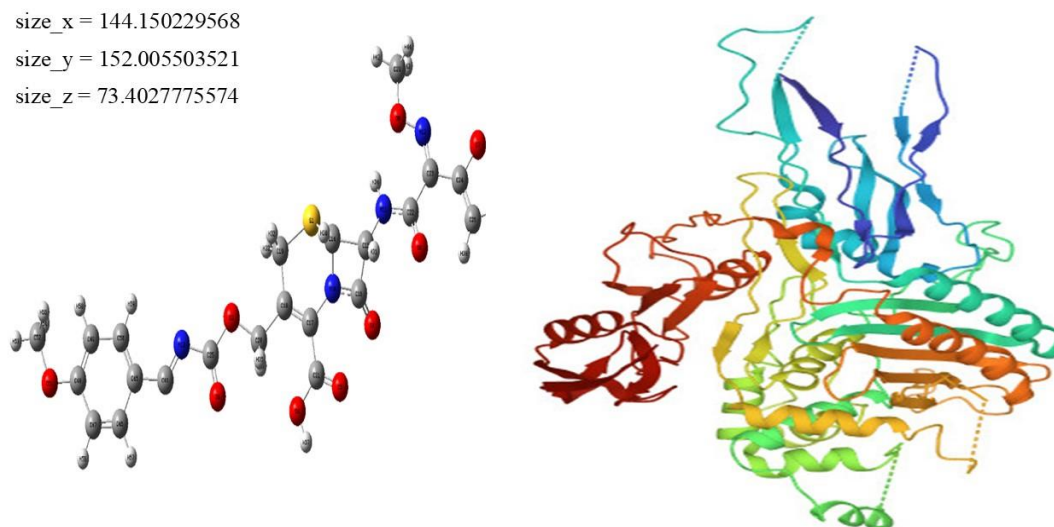


Figure 3: 3D structure of SB ligand p-anisalcefuroxime (a) and 3D structure of PBP2x (b)

Statistical analysis: One-way analysis of variance (ANOVA) was used to evaluate the data, reporting the results with mean±SEM. Tukey's multiple range test was used to find significant differences between the means at $p < 0.05$.

Results

Physical states, melting points, and solubility measurements: The yield, colour, and melting point of the prepared SB ligand p-anisalcefuroxime was 88.0%, orange yellowish and above 225°C. It showed solubility nature in methanol, and ethanol, however, it was not soluble in chloroform and acetone.

Identification test of SB ligand: **Table 1** presents the results of various identification tests performed on the SB ligand, confirming the presence or absence of specific functional groups. The phenolic group test showed no violet colour formation, indicating the absence of a phenolic group. The carboxylic group test resulted in bubble formation, confirming the presence of a carboxylic group. The primary amine test did not produce a reddish-orange precipitate, indicating the absence of a primary amine group. The aldehyde group test also showed no red colour, confirming the absence of an aldehyde group. These results help in understanding the ligand's chemical structure and functional properties.

Table 1: Identification test of Schiff base ligand

Test	Name of the test	Observations	Results
Phenolic group test	(Sample+ ethanol+ Ferric Chloride) added together	Violet color was not formed	Phenolic group absent
Carboxylic group test	Sample in watch glass, NaHCO ₃ was added	Bubble was formed	Carboxylic group is present
Primary amine test	Sample+ dil. HCl + boil and cool+ NaNO ₂ solution in NaOH	Reddish-orange ppt. was not formed	Absence of primary amine group
Aldehyde group test	Sample+ Fehling A+ Fehling B	Red Color is not observed	Absence of aldehyde group

(+) = Identification test of SB ligand

Table 2: Identification test of metal complexes

Test	Observations	Results
Copper Sulfate Test Sample+ few drops of sodium hydroxide solution	Formation of blue precipitate	Presence of Cu ²⁺
Ferrous Sulfate Test Prepare Solution with Methanol (substances can be identified by their colors)	Green color is observed	Presence of Fe ²⁺

R_f values measurement for SB ligand: The TLC and R_f value of SB ligands were measured by using the solvent (10:4) n-hexane: CHCl₃. (1) R_f value of cefuroxime [Active] was 0.03 mm, (2) R_f value of the SB ligand was 22 mm, (3) R_f value of anisaldehyde 21 mm.

R_f values measurement for metal complexes: The TLC and R_f value of Metal Cu²⁺ and Fe²⁺ were measured by using the solvent (10: 4) n-hexane: CHCl₃ and (10: 6) n-hexane: CHCl₃.

UV-spectral analysis of SB ligand: The electronic absorption spectra are often very helpful in the evaluation of results furnished by other methods of structural investigation. The electronic spectral measurements were used for assigning the stereochemistry of ligands based on the positions and number of d-d transition peaks.²⁰ The electronic absorption spectra of the SB ligand p-anisalcefuroxime and cefuroxime were recorded at a room temperature using methanol as solvent. The absence of any band above 400 nm for the prepared complex indicates that it does not exhibit any d-d transition. The band observed below 400 nm for the complex is due to the intraligand π-π* and n-π* transitions. The bands appearing around 400 nm are due to charge transfer absorptions tailing from the ultraviolet.

UV-spectral analysis of metal complexes

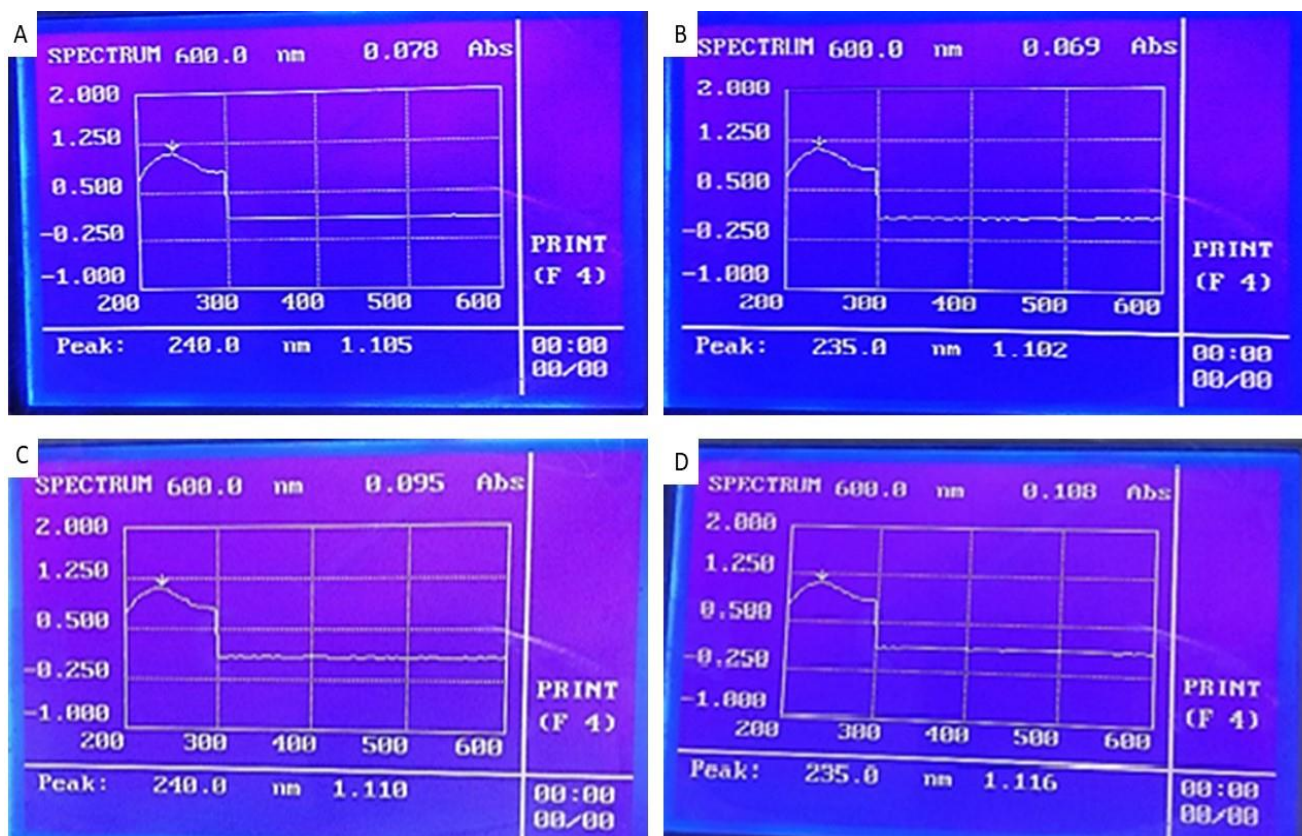


Figure 4: UV spectrum of SB ligand (A), cefuroxime (B), Cu²⁺ complex (C), and Fe²⁺ complex (D)

R_f value of cefuroxime [active] was 0.03 mm, the SB ligand was 22 mm and Cu^{2+} SB ligand complex was 18 mm), and Fe^{2+} metal complex was 12 mm.

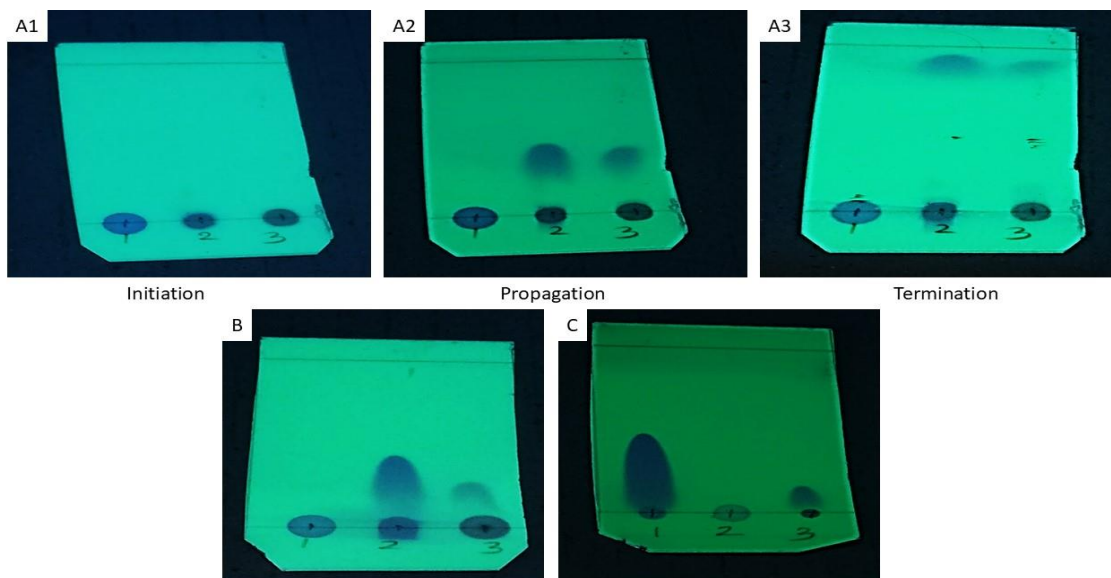


Figure 5: R_f value determination of SB ligand (A1, A2, and A3), Cu^{2+} complex (B), and Fe^{2+} complex (B)

^1H NMR Spectral analysis: From the ^1H NMR spectrum of the SB ligand p-anisalcefuroxime we found a broad singlet signal at δ 8.18 ppm for the azomethine ($-\text{N}=\text{CH}-$) proton. Multiple signals found at δ 5.1-5.5 ppm for 1-amide. From the ^1H NMR spectrum of the SB ligand p-anisalcefuroxime we found broad peak at δ 12.56 ppm for ($-\text{COOH}$) group and a singlet peak was found in δ 4.83 ppm for $[-\text{CH}_2]$. It was indicated that the azomethine group shows a characteristic shift in the vicinity of δ 7.0-8.0 ppm, as claimed by ^1H NMR spectra of some azomethines.

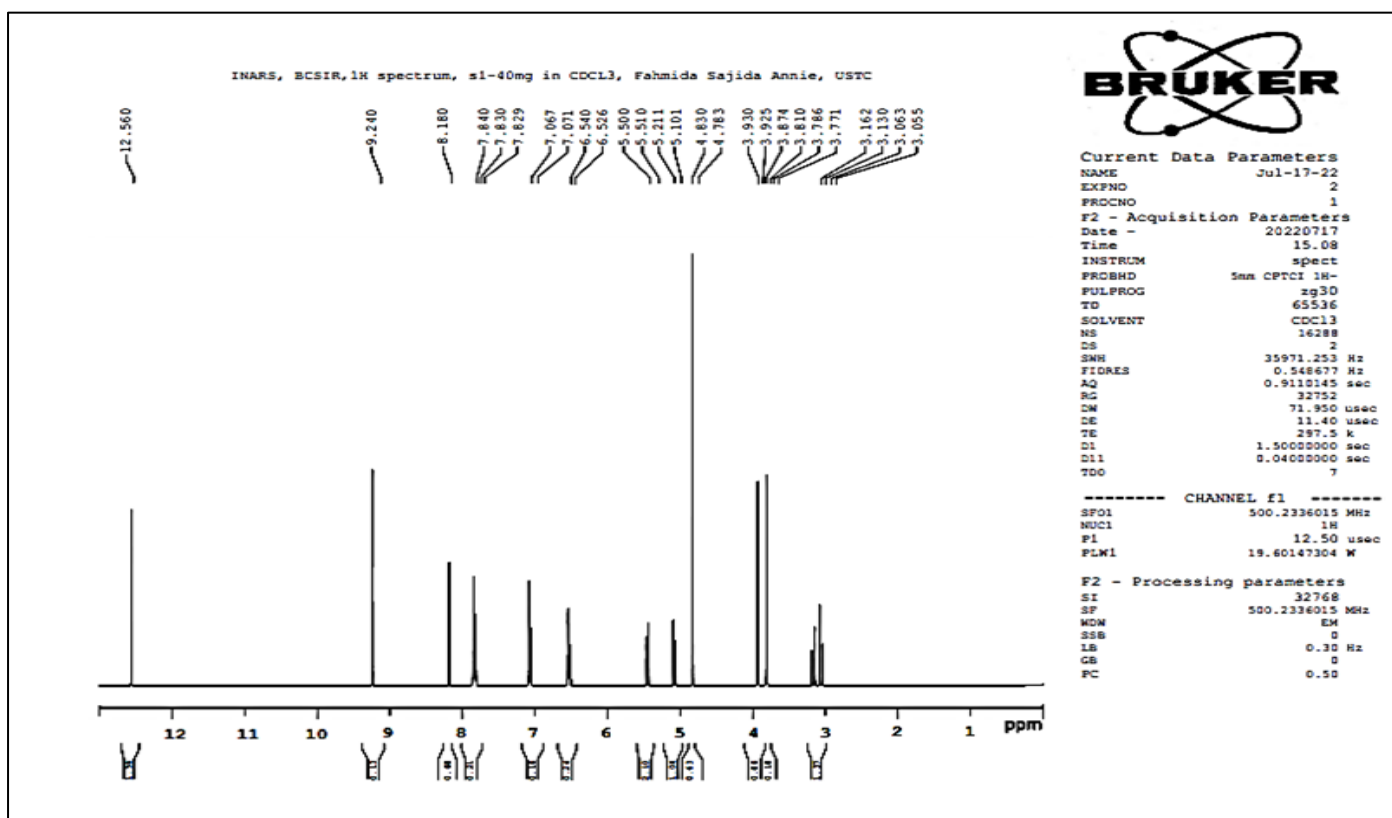


Figure 6: ^1H NMR spectral analysis of SB ligand p-anisalcefuroxime

Table 3 presents the ^1H NMR spectral analysis of the SB ligand p-anisalcefuroxime, showing the chemical shifts (in ppm) along with proton assignments. This data provides detailed insights into the structure of the compound and the types of hydrogen atoms within its molecular framework. The δ 12.56 ppm chemical shift corresponds to a singlet (S), 1H signal, which is attributed to the carboxyl proton (-COOH), typical of carboxylic acid groups [13]. The presence of this acidic proton is crucial for understanding the compound's ability to form salts or participate in hydrogen bonding, enhancing its biological activity. At δ 3.93 ppm and 3.81 ppm, two singlet (S), 3H signals are observed, which are assigned to the methoxy groups (-OCH₃) on a phenyl ring (Ph-OCH₃) and on a nitrogen atom (N-OCH₃), respectively. These signals confirm the presence of methoxy substitution on both the aromatic ring and nitrogen, which could influence the compound's lipophilicity and its interaction with biological targets [14]. The signal at δ 8.18 ppm corresponds to a singlet (S), ^1H proton, assigned to the SB (-N=CH-) linkage, which is characteristic of imines. SBs are commonly involved in metal coordination, suggesting the compound's potential for forming metal complexes [15]. The range δ 5.1-5.5 ppm contains a multiple corresponding to 4H, assigned to the amine protons (-NH-), indicative of an amide or amine linkage in the structure. This proton environment supports the presence of nitrogen-based functional groups.

Further, the aromatic region includes signals at δ 7.84, 6.54, and 6.53 ppm, which are attributed to 3H protons from the furan ring (Furan-H). These protons suggest the presence of a furan ring, a characteristic feature in many biologically active compounds [16]. Also, the two signals at δ 7.07 ppm and 7.83 ppm correspond to 2H each, assigned to aromatic protons of the phenyl ring (Ph-H), indicating the presence of a benzene ring in the structure. Finally, the signals at δ 3.06 ppm and 3.16 ppm correspond to 2H each, assigned to methine (-CH₂) and sulfur methylene (S-CH₂) protons, respectively, while the signal at δ 4.83 ppm is attributed to 2H of a methylene group (-CH₂), contributing further to the overall structure. In conclusion, the ^1H NMR data of p-anisalcefuroxime confirms the presence of key functional groups, including a carboxylic acid, methoxy groups, amide linkages, a SB, and a furan ring, all of which contribute to the compound's potential biological and chemical properties.

Table 3: ^1H NMR spectral analysis of Schiff base ligand p-anisalcefuroxime

Compound	Chemical shift δ (in ppm)	Assignment of protons
p-anisalcefuroxime	12.56	S, 1H, [-COOH]
	3.93	S, 3H, [Ph-OCH ₃]
	3.81	S, 3H, [N-OCH ₃]
	8.18	S, 1H, [-N=CH-]
	5.1-5.5	S, 4H, [-NH-]
	7.84, 6.54, 6.53	S, 3H, [Furan-H]
	7.07	S, 2H, [Ph-H]
	7.83	S, 2H, [Ph-H]
	3.06	S, 2H, [S-CH ₂]
	3.16	S, 2H, [S-CH ₂]
4.83	S, 2H, [-CH ₂]	

^{13}C NMR Spectral analysis: From the NMR spectrum of the SB ligand p-anisalcefuroxime we found a broad singlet signal at δ 163.7 ppm for the azomethine (-N=CH-) proton. Solvent Chloroform shows signal at δ 77.01 ppm. From the ^{13}C NMR spectrum of the SB ligand p-anisalcefuroxime we found broad peak at δ 161.9 ppm for (-COOH) group.

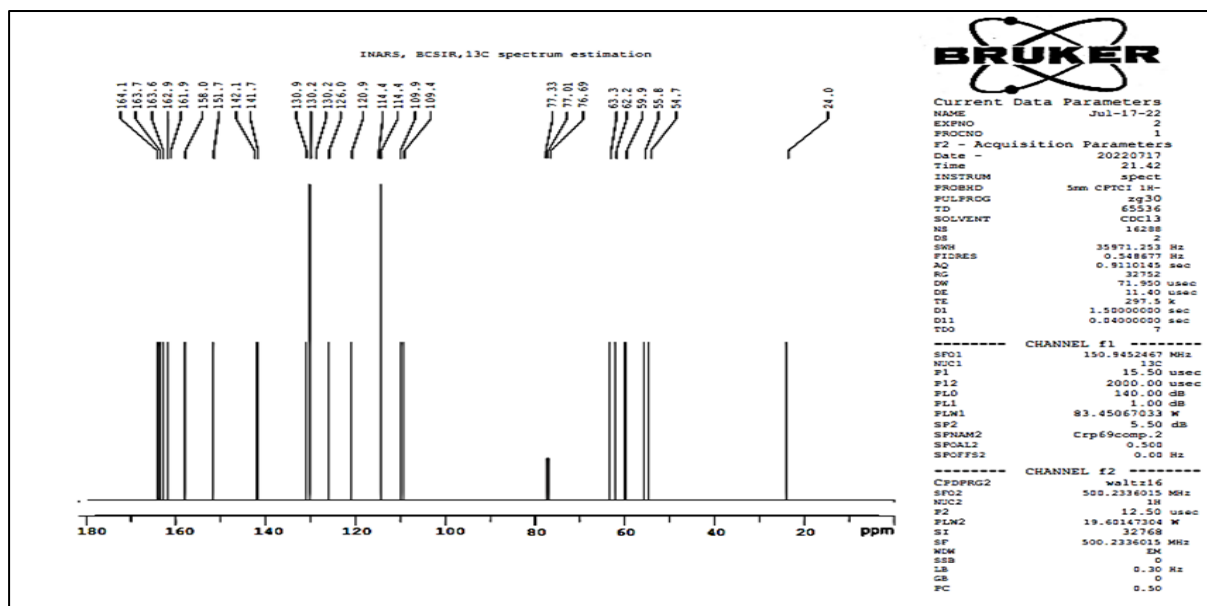


Figure 7: ^{13}C NMR spectral analysis of Schiff base ligand p-anisalcefuroxime

Table 4 presents the ^{13}C NMR spectral analysis of the SB ligand p-anisalcefuroxime, detailing the chemical shifts δ (in ppm) and corresponding proton assignments. This analysis provides valuable information about the molecular structure and functional groups present in the compound.

Table 4: ^{13}C NMR spectral analysis of Schiff base ligand p-anisalcefuroxime

Compound	Chemical shift δ (in ppm)	Assignment of protons
p-anisalcefuroxime	109.4, 109.9, 141.7, 142.1	4C, [Furan-2]
	161.9	1C, [-COOH]
	163.6, 164.1	2C, [R-CO-NH ₂]
	120.9, 130.9	2C, [H ₂ C=CH ₂]
	163.7	1C, [-CH=N-]
	77.01	[CDCl ₃]
	59.9, 62.2	2C, [-CH]
	24.0, 54.7	2C, [-CH ₂]
	55.8, 63.3	2C, [-CH ₃]

The chemical shifts at δ 109.4, 109.9, 141.7, and 142.1 ppm are attributed to the carbon atoms in the furan-2 ring (4C). These signals indicate the presence of aromatic carbons involved in conjugation with the rest of the structure. The δ 161.9 ppm shift corresponds to the carbonyl group of a carboxylic acid (-COOH) functional group (1C), confirming the presence of an acidic moiety in the compound. At δ 163.6 and 164.1 ppm, the signals correspond to carbonyl carbons attached to amino (-NH₂) groups, likely forming part of an amide functional group, as indicated by the R-CO-NH₂ assignment (2C). This suggests the compound contains amide linkages, important for its biological activity. The δ 120.9 and 130.9 ppm shifts represent carbons involved in an alkene group (-CH₂=CH₂) (2C), highlighting the presence of a double bond in the structure, which contributes to the compound's conjugation and potentially affects its reactivity and interaction with biological targets. The δ 163.7 ppm signal is indicative of a -CH=N- group (1C), suggesting the presence of a SB linkage, which is common in coordination chemistry and could contribute to the ligand's ability to form complexes with metal ions. The signals at δ 77.01 ppm correspond to CDCl₃, the solvent used in the NMR analysis, while the signals at δ 59.9, 62.2 ppm (2C) and 24.0, 54.7 ppm (2C) represent -CH and -CH₂ groups, respectively.

Finally, the δ 55.8, 63.3 ppm signals correspond to methyl ($-\text{CH}_3$) groups (2C), indicating the presence of alkyl groups that may affect solubility and steric interactions. This ^{13}C NMR data confirms the structural complexity of p-anisalcefuroxime, with key functional groups such as furan, carboxylic acid, amide, alkene, and SB, all contributing to its overall molecular properties.

IR Spectral analysis: All IR spectra of the SB ligand p-anisalcefuroxime was recorded using KBr-discs in the IR spectra of SB ligand p-anisalcefuroxime and both complexes Cu^{2+} and Fe^{2+} displays the characteristic bands at 1598, 1600, 1600 cm^{-1} for azomethine ($-\text{N}=\text{CH}-$) group; 2359 cm^{-1} for carboxylic group ($-\text{COOH}$); and 1154, 1159, 1158 cm^{-1} for $-\text{OCH}_3$. IR spectral analysis of the SB ligand and metal complexes (**Table 5**).

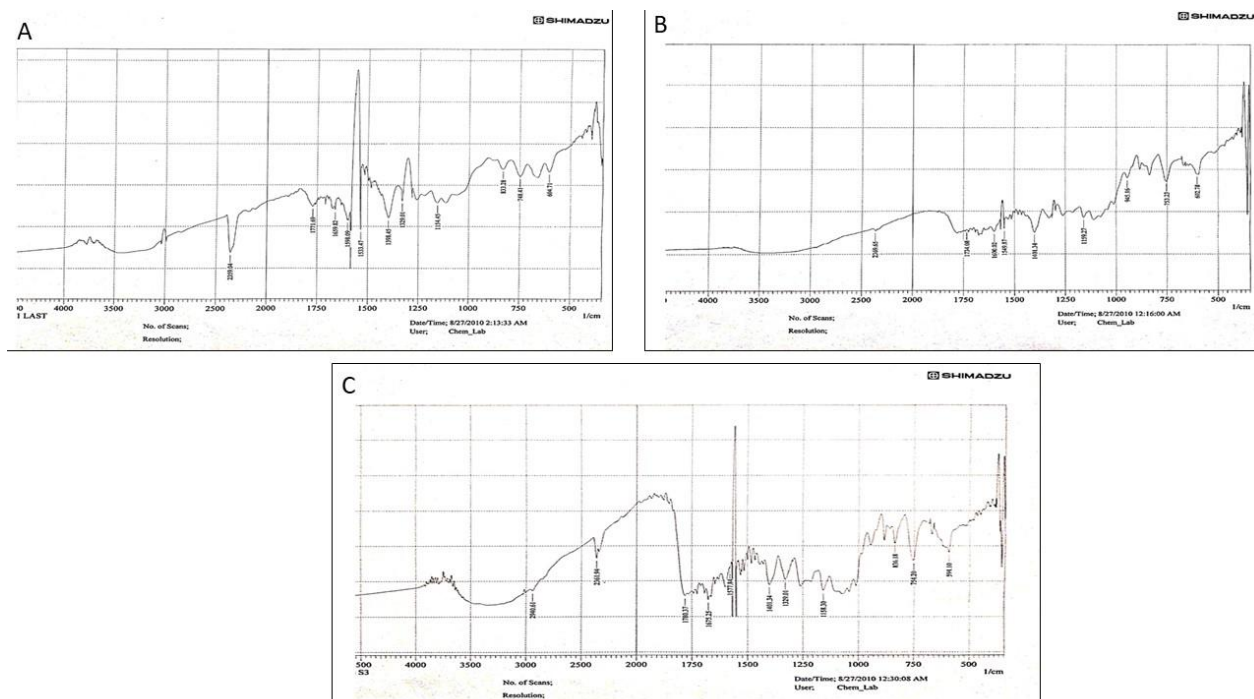


Figure 8: IR analysis of SB ligand of p-anisalcefuroxime (A), Cu^{2+} complex (B), and Fe^{2+} complex (C)

Table 5: IR spectral analysis of the Schiff base ligand and metal complexes

Compound	$-\text{N}=\text{CH}-$ cm^{-1}	$-\text{COOH}$ cm^{-1}	Coupling of Benzene ring cm^{-1}	$\text{C}=\text{O}$ cm^{-1}	$\text{C}-\text{N}$ cm^{-1}	$-\text{OCH}_3$ cm^{-1}
p-anisalcefuroxime	1598	2359	1533, 1398	1771,1659	1329	1154
Cu^{2+} complex	1600	2369	1549, 1401	1734,1645	1318	1159
Fe^{2+} complex	1600	2361	1545, 1401	1780,1675	1329	1158

Antibacterial activity of SB ligand p-anisalcefuroxime and its metal complex: **Table 6** presents the antibacterial activity of SB-Ligand p-anisalcefuroxime and its metal complexes (Cu^{2+} & Fe^{2+}) against various bacterial strains, as measured by the zone of inhibition in millimetres (mm) at a concentration of 5 mg/ml. The data provides insight into the antimicrobial potential of both the ligand and its metal complexes. The results show that p-anisalcefuroxime (A1) demonstrates antibacterial activity against several bacterial strains. For example, it exhibited a 17 mm zone of inhibition against *S. aureus* (gram-positive), which indicates moderate antibacterial activity. The Cu^{2+} complex (A2) showed a 13 mm zone against *S. aureus*, while the Fe^{2+} complex (A3) exhibited a slightly stronger inhibition at 18 mm. This suggests that the iron complex might enhance the antibacterial efficacy of the ligand [17, 18], likely due to the metal's role in facilitating interaction with bacterial cell structures, as metal ions can influence the binding of ligands to bacterial targets [19].

Table 6: Antibacterial activity of Schiff base Ligand *p*-anisalcefuroxime and its metal complex

Test Organisms	Zone of Inhibition (5mg/ml)			
	Sample (mm) A ₀	SB-Ligand(mm) A ₁	Complex Cu ²⁺ (mm) A ₂	Complex Fe ²⁺ (mm) A ₃
<i>S. aureus</i> (+ve)	22	17	13	18
<i>E. Coli</i> (-ve)	20	13	7	08
<i>S. Typhi</i> (-ve)	10	N/A	N/A	N/A
<i>K. pneumonia</i> (-ve)	18	13	N/A	10

A0=cefuroxime sample (mm), A1=*p*-anisalcefuroxime SB-ligand (mm), A2=complex Cu²⁺ (mm), A3=complex Fe²⁺ (mm)

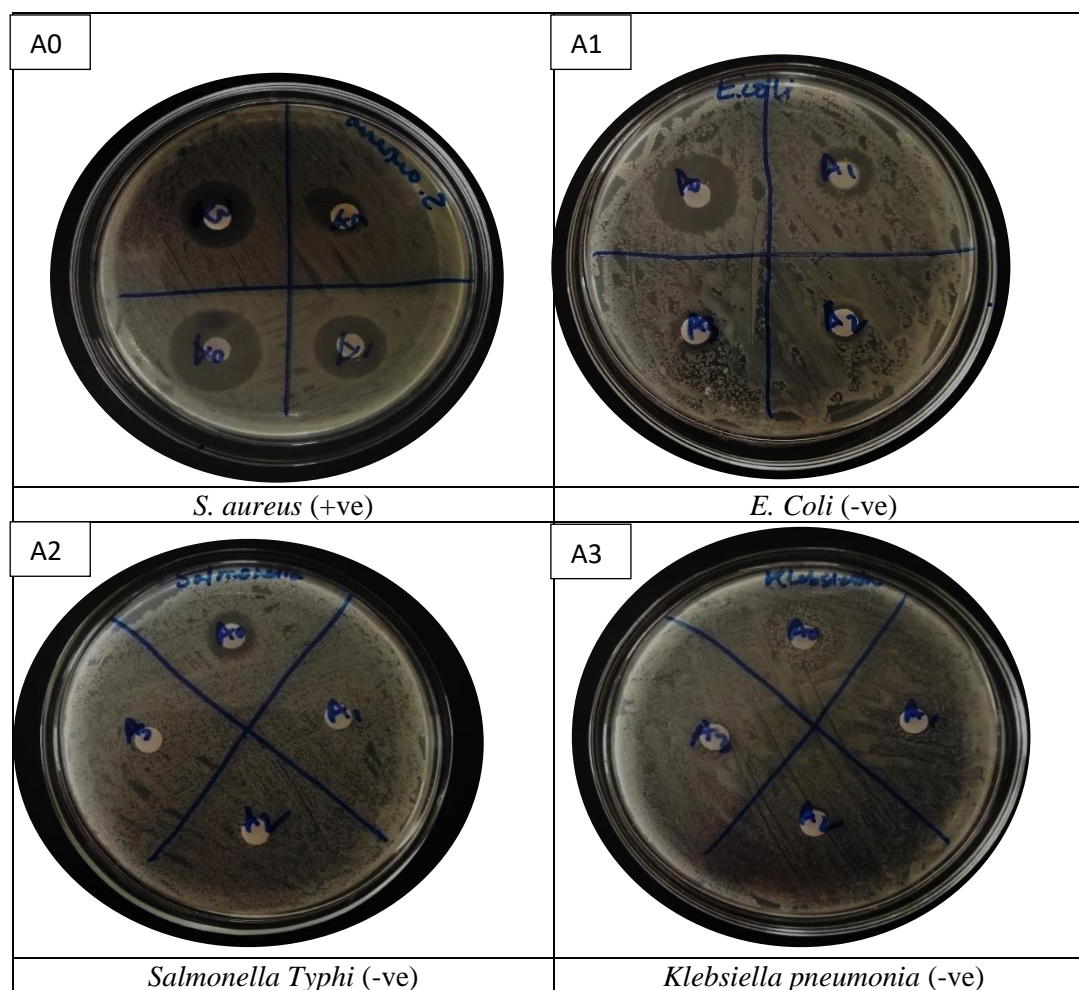


Figure 9: Antibacterial activity of SB ligand *p*-anisalcefuroxime and its metal complex

A0=cefuroxime sample (mm), A1=*p*-anisalcefuroxime SB-ligand (mm), A2=complex Cu²⁺ (mm), A3=complex Fe²⁺ (mm)

Khan and others [20] utilized both experimental and computational methods to evaluate the antibacterial activity of *Urtica dioica* essential oil. The antibacterial effects were assessed through disk diffusion and broth microdilution methods, followed by molecular docking simulations to identify potential bioactive compounds responsible for the observed activity. Azad and others [21] assessed the antimicrobial activity of *Cuscuta reflex* Roxb. extracts *in-vitro* using the agar well diffusion method, followed by minimum inhibitory concentration (MIC) determination. Similarly, the current study followed by the same technique which consider to achieve reasonable growth of inhibition. The study involved evaluating the extracts against a variety of bacterial strains to determine their antibacterial efficacy. Azarbarani and others [22] conducted antimicrobial testing on essential oils from *Ferulago macrocarpa* flower and leaf extracts using disk diffusion, broth microdilution, and agar dilution techniques. The study also included the determination of MIC values to

assess the potency of the essential oils against a range of bacterial and fungal pathogens. Just as these studies utilized experimental methods like disk diffusion, broth microdilution, and agar dilution to evaluate antimicrobial properties, the present study also investigates the antibacterial potential of SB complexes using similar techniques against both gram-positive and gram-negative bacterial strains. Additionally, the computational approach used in the current study, including molecular docking with PBP2x of *Streptococcus pneumoniae*, parallels the computational analyses in the referenced studies, where molecular docking was employed to identify key bioactive compounds responsible for antimicrobial effects. Both experimental and computational methods combined enhance the understanding of the antibacterial mechanisms of these compounds, showing their potential as promising leads for new drug development. Recent study reported that SBs were synthesized by condensing 5-aminopyrazoles with aromatic aldehydes and evaluated for their *in vitro* antibacterial activity against multi-drug-resistant bacteria (MDRB), showing promising results. In addition, molecular docking studies indicated potential kinase inhibition against *Staphylococcus aureus* DNA gyrase and dihydrofolate reductase enzymes. Additionally, the compounds adhered to Lipinski's rule and exhibited favorable drug-like properties, suggesting their potential as lead candidates for new antibiotic development [23]. Several SB metal complexes demonstrated *in vitro* antimicrobial activities comparable to or exceeding that of reference drugs. Their known anticorrosive properties, combined with antimicrobial efficacy, suggest potential applications in various types of surgeries. These findings highlight SB metal complexes as promising candidates for addressing antibiotic resistance and warrant further exploration in medicinal chemistry and catalysis [24]. The studies reviewed highlight the promising antibacterial potential of SB complexes, with both experimental and computational approaches demonstrating significant antimicrobial activity. Techniques like disk diffusion, broth microdilution, and molecular docking were employed to evaluate these compounds' efficacy against various bacterial strains, including MDRB. SB metal complexes, with their favourable drug-like properties and anticorrosive potential, show promise as candidates for addressing antibiotic resistance. These findings suggest that SB complexes could serve as valuable leads for the development of new antibiotics and other therapeutic applications.

Molecular docking analysis: The maximum level of energy release at -7.3. As we know the highest the negative score showed the better orientation means more binding affinity.

Table 7: Binding affinity (kcal/mol) of Schiff base ligands and its analogues

Ligand Docking Pose	Binding Affinity (kcal/mole)	rmsd/ub	rmsd/lb
D0	-7.3	0	0
D1	-7.1	2.301	1.822
D2	-7.1	74.201	71.004
D3	-7.1	101.755	97.443
D4	-7.1	98.539	94.241
D5	-6.9	41.88	39.165
D6	-6.9	80.492	75.144
D7	-6.9	82.756	75.668
D8	-6.8	94.018	90.65

The binding affinity values presented in **Table 7** reflect the strength of interaction between SB ligands and their respective target proteins, with more negative binding affinity scores indicating stronger interactions. In this context, the ligand D0 demonstrates the most favourable binding affinity at -7.3 kcal/mol, indicating optimal molecular orientation and a stronger ligand-target binding interaction. A more negative score correlates with better orientation in the binding site, suggesting that D0 may have the highest binding affinity, which is essential for therapeutic efficacy [25]. Ligands D1 to D8 exhibit binding affinities ranging from -7.1

kcal/mol to -6.8 kcal/mol. These values, though slightly higher (less negative), still suggest relatively strong binding, but less so than D0. Ligands D1, D2, D3, D4, and D5 show a consistent binding affinity of -7.1 kcal/mol or -6.9 kcal/mol, indicating similar potential interactions, though the variations in their root-mean-square deviation (rmsd) values offer further insight into the stability of their docking poses.

The rmsd/ub (unbound) and rmsd/lb (bound) values measure the flexibility and stability of the docking pose, where lower values indicate a more stable conformation. For D0, the rmsd values are 0, both unbound and bound, which indicates a stable, rigid docking pose with minimal flexibility. This supports its strong binding affinity. In contrast, ligands like D2 and D3 show high rmsd values (e.g., 74.201 and 101.755 for rmsd/ub) and larger discrepancies between unbound and bound poses. This suggests that their binding poses are less stable and more flexible, which could reduce their effectiveness compared to D0. The overall trend in **Table 8** suggests that while all the ligands have promising binding affinities, D0 stands out due to its stronger interaction with the target and stable docking pose. In drug design, both binding affinity and pose stability are crucial for the development of effective therapeutics [26-27].

Physicochemical properties: The pink area represents the optimal range for each property here the compound is predicted not orally bioavailable, because too flexible and too polar.

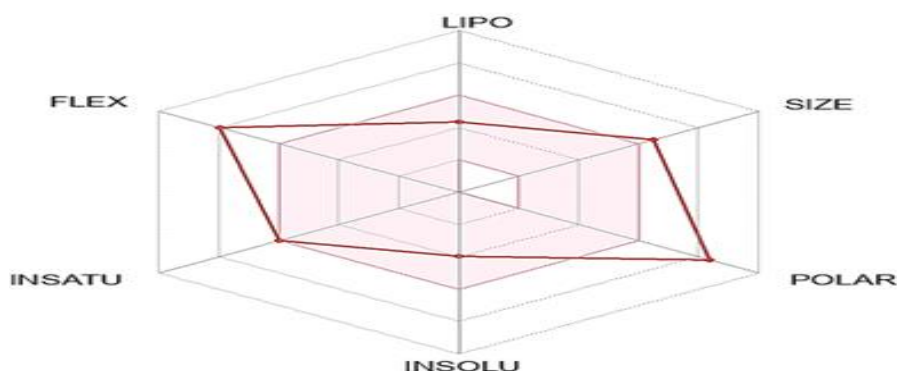


Figure 10: Bioavailability radar enables a first glance at the drug-likeness of a molecule

Figure 10, the bioavailability radar, suggests that the compound falls outside the optimal range for oral bioavailability. The pink area highlights the ideal properties for drug-likeness, but the compound's characteristics, such as excessive flexibility and polarity, place it outside this range. This indicates that the compound may face challenges in terms of gastrointestinal absorption and systemic availability when taken orally. Its high flexibility and polarity could hinder its ability to cross biological membranes effectively, reducing its potential as an orally bioavailable drug. Thus, improvements in its physicochemical properties may be needed for better bioavailability.

Pharmacokinetics parameters study: The pharmacokinetics parameters in **Table 8** suggest that the compound has low GI absorption, with only 57% absorbed, indicating limited bioavailability through the gastrointestinal tract. It is not permeant to the blood-brain barrier (BBB), which may limit its central nervous system (CNS) effects. Skin permeability is also low, suggesting minimal absorption through the skin. The compound is a CYP2C9 inhibitor, which could affect the metabolism of other drugs metabolized by this enzyme, leading to potential drug interactions. It is a P-glycoprotein substrate, meaning it may be actively transported out of cells, potentially affecting its distribution and absorption. Its bioavailability score of 0.11 suggests poor overall absorption or systemic availability. With moderate water solubility (-3.5 log mol/L), the compound has limited solubility in aqueous environments. The total clearance is relatively low, indicating slow elimination. Hepatotoxicity is a concern, and the maximum tolerated dose in humans is 0.375 mg/kg/day.

Table 8: Representing the pharmacokinetics parameters of respective compounds

Property	Predicted Value
GI absorption	57.003 (% Absorbed) Low
BBB permeant	No
Skin Permeability	Low
CYP2C9 inhibitor	Yes
P-glycoprotein substrate	Yes
Bioavailability Score	0.11
Water solubility	-3.5 (log mol/L) Moderately soluble
Total Clearance	0.164
Hepatotoxicity	Yes
Max. tolerated dose (human)	0.375 mg/kg/day

p-anisalcefuroxime boiled egg figure study: The boiled egg figure study of p-anisalcefuroxime (**Figure 11**) suggests that the compound has no potential for blood-brain barrier (BBB) penetration, indicating it is unlikely to affect the central nervous system. It may also have low gastrointestinal (GI) absorption, limiting its bioavailability after oral administration. Additionally, the study highlights a potential risk for hepatotoxicity, which could affect liver function. The maximum tolerated dose is 0.375 mg/kg/day, suggesting a low tolerance for higher dosages, possibly due to toxicity concerns. These findings indicate that while the compound may have therapeutic effects, its safety profile requires careful consideration.

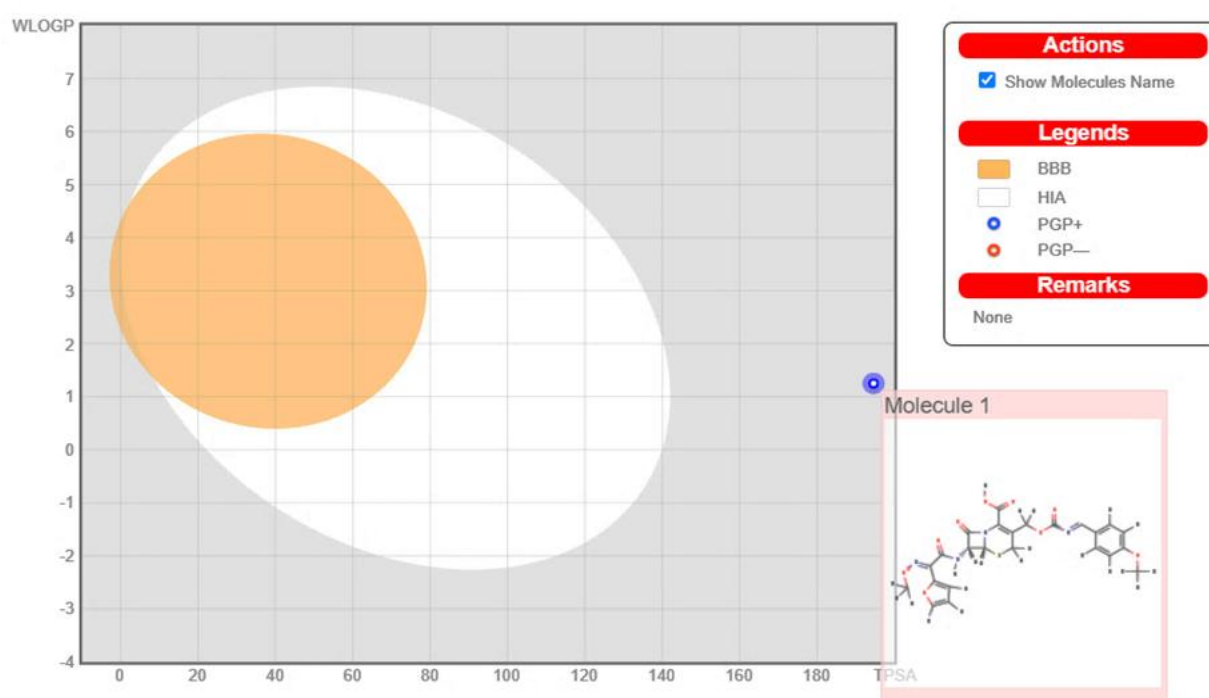


Figure 11: p-anisalcefuroxime boiled egg figure study

Discussion

The study explored the synthesis of a novel SB ligand, derived from p-anisaldehyde and cefuroxime, resulting in the formation of a SB, which was further coordinated with metal ions of Cu^{2+} and Fe^{2+} to form metal complexes. These metal complexes were subjected to extensive characterization using a variety of techniques, including IR, NMR spectroscopy (^1H NMR and ^{13}C NMR), UV spectroscopy, melting point determination, chemical tests, Thin-Layer Chromatography (TLC) analysis, colour tests, and solubility assessments. The data confirmed the successful formation of SB ligands and their corresponding metal complexes. The antibacterial activity of the synthesized complexes was evaluated against a range of bacterial strains, both gram-positive

and gram-negative, demonstrating promising antibacterial properties. This suggests that the Cu^2 and Fe^{2+} metal complexes of the SB ligand have the potential to be developed into effective antibacterial agents. The study's results are consistent with the known properties of transition metal complexes, which are often highly effective in biological applications due to their favourable biocompatibility, low toxicity, and ability to interact with biomolecules.

Pharmacokinetic parameters of SB ligands, such as p-anisalcefuroxime when complexed with metal ions like Cu^2 and Fe^{2+} , are critical in determining their therapeutic potential, efficacy, and safety profile. SBs, particularly those complexed with metal ions, can exhibit altered pharmacokinetic properties due to changes in their solubility, permeability, and bioavailability. The following aspects of pharmacokinetics are relevant for understanding how SB metal complexes might behave *in vivo*. SB ligands often have limited solubility in aqueous environments due to their relatively hydrophobic nature, which can limit their absorption through the gastrointestinal (GI) tract. However, when complexed with metal ions such as Cu^2 and Fe^{2+} , the solubility of SB complexes can be enhanced, potentially improving their absorption. Metal chelation might increase the bioavailability by altering the physicochemical properties of the compound, facilitating easier crossing of cell membranes. Nonetheless, bioavailability may still be limited by other factors such as first-pass metabolism or poor permeability [28]. The ability of SB metal complexes to cross the blood-brain barrier (BBB) is crucial for their potential to treat central nervous system disorders. Complexes with metal ions like Cu^2 may exhibit enhanced interaction with proteins involved in the transport across the BBB, but whether they can efficiently permeate depends on their size, lipophilicity, and the metal's influence on their structure. Cu^{2+} complexes may also exhibit redox properties that could alter their interaction with the BBB, influencing both therapeutic and toxicological outcomes [29]. SB metal complexes like p-anisalcefuroxime with Cu^2 and Fe^{2+} ions exhibit promising antimicrobial activity. Metal ions can act as a catalytic centre, enhancing the interaction of the complex with microbial cell membranes, leading to disruption and inhibition of growth. These complexes often show potent activity against multi-drug-resistant bacteria, highlighting their potential as antibacterial agents [30, 31]. SB metal complexes, such as those containing Cu^2 and Fe^{2+} ions, have shown promising pharmacokinetic characteristics, including enhanced solubility and potential for antimicrobial efficacy. However, their bioavailability, BBB permeability, and cytochrome P450 interactions require further investigation to optimize their therapeutic applications and minimize risks of toxicity or drug-drug interactions. Future research should focus on improving their pharmacokinetic properties and evaluating their safety and efficacy in clinical settings. Cytochrome P450 enzymes, including CYP2C9, play a significant role in the metabolism of many drugs. SB metal complexes, especially those with Cu^2 and Fe^{2+} , can potentially inhibit or induce certain CYP enzymes. This interaction could lead to drug-drug interactions, altering the metabolism of other substrates. For example, Cu^{2+} complexes could inhibit the activity of CYP enzymes, leading to altered pharmacokinetics and possible accumulation or increased toxicity of co-administered drugs [32]. Further investigation was conducted using molecular docking studies, specifically docking the SB ligands with PBP2x of *Streptococcus pneumoniae*. This analysis revealed that the SB ligand showed a strong binding affinity, indicating that the ligand may interact effectively with the target enzyme, supporting its potential as a lead compound in the development of antibacterial drugs targeting bacterial cell wall synthesis. The pharmacokinetic properties of the SB ligand were also assessed using online web tools such as Swiss ADME, pkCSM, and admetSAR. The results suggested that the SB ligand exhibited favourable absorption, distribution, metabolism, and excretion properties, which are crucial for the design of viable drug candidates. The ligand's profile indicated it may have a good bioavailability and low toxicity, further enhancing its potential as a therapeutic agent. The main limitation of this study is the synthesised compounds not investigated in details characterization and not tested for bioactivity in *in-vivo* and also not performed toxicity study. However, future research could focus on optimizing the synthesis, exploring additional metal ions, and conducting *in vivo* studies to further validate the therapeutic potential of these complexes.

Conclusion: The synthesized Schiff base ligand and its metal complexes exhibit significant antibacterial activity and promising pharmacokinetic properties, making them strong candidates for further development as antibacterial agents. The coordination of the Schiff base with transition metals not only enhances its biological activity but also opens up avenues for the design of novel metal-based therapeutics.

References

1. Asghar AA, Akhlaq M, Jalil A, Azad AK, Asghar J, Adeel M, Abdel-Daim MM (2022) Formulation of ciprofloxacin-loaded oral self-emulsifying drug delivery system to improve the pharmacokinetics and antibacterial activity. *Frontiers in Pharmacology*. 13: 967106. doi: 10.3389/fphar.2022.967106
2. Thønnings S, Jensen KS, Nielsen NB, Skjønnemand M, Hansen DS, Lange KHW, Frimodt-Møller N (2020) Cefuroxime pharmacokinetics and pharmacodynamics for intravenous dosage regimens with 750 mg or 1500 mg doses in healthy young volunteers. *Journal of Medical Microbiology*. 69 (3): 387-395. doi: 10.1099/jmm.0.001138.
3. Theuretzbacher U (2017) Global antimicrobial resistance in gram-negative pathogens and clinical need. *Current Opinion in Microbiology*. 39: 106-112. doi: 10.1016/j.mib.2017.10.028
4. Al Zoubi W (2013) Biological activities of Schiff bases and their complexes: A review of recent works. *International Journal of Organic Chemistry*. 3 (3A): 73-95. doi: 10.4236/ijoc.2013.33A008
5. Iacopetta D, Ceramella J, Catalano A, Mariconda A, Giuzio F, Saturnino C, Longo P, Sinicropi MS (2022) Metal complexes with Schiff bases as antimicrobials and catalysts. *Inorganics*. 11 (8): 320. 1-28. doi: 10.3390/inorganics11080320
6. Karges J, Stokes RW, Cohen SM (2021) Metal complexes for therapeutic applications. *Trends in Chemistry*. 3 (7): 523-534. doi: 10.1016/j.trechm.2021.03.006
7. Jaber QA, Shentaif AH, Almajidi M, Ahmad I, Patel H, Azad AK, Rao SA (2023) Synthesis, structure, and in vitro pharmacological evaluation of some new pyrimidine-2-sulfonamide derivatives and their molecular docking studies on human estrogen receptor alpha and CDK2/Cyclin proteins. *Russian Journal of Bioorganic Chemistry*. 49 (Suppl 1): S106-S118. doi: 10.1134/S1068162023080095
8. Arifuzzaman M, Karim MR, Siddiquee TA, Mirza AH, Ali MA (2013) Synthesis and characterization of new Schiff bases formed by condensation of 2, 9-phenanthroline-1, 10-dialdehyde with sulfur-containing amines. *International Journal of Organic Chemistry*. 3 (1): 81-86. doi: 10.4236/ijoc.2013.31009
9. Azad AK, Sulaiman WMAW, Almoustafa H, Dayoob M, Kumarasamy V, Subramaniyan V, Khan AA (2024) A dataset of microstructure features of electro-hydrodynamic assisted 5-fluorouracil-grafted alginate microbeads and physicochemical properties for effective colon targeted carriers drug delivery. *Data in Brief*. 53: 110202. doi: 10.1016/j.dib.2024.110202
10. Silverstein RM, Webster FX, Kiemle DJ, Bryce DL (2014) *Spectrometric identification of organic compounds* (8th ed.). Wiley-Interscience. ISBN: 978-0-470-61637-6.
11. Sharma B, Shukla S, Rattan R, Fatima M, Goel M, Bhat M, Dutta S, Ranjan RK, Sharma M (2022) Antimicrobial agents based on metal complexes: present situation and future prospects. *International Journal of Biomaterials*. 2022: 6819080. doi: 10.1155/2022/6819080
12. Daina A, Michielin O, Zoete V (2017) SwissADME: a free web tool to evaluate pharmacokinetics, drug-likeness and medicinal chemistry friendliness of small molecules. *Scientific Reports*. 7 (1): 42717. doi: 10.1038/srep42717
13. Zloh M (2019) NMR spectroscopy in drug discovery and development: Evaluation of physico-chemical properties. *ADMET DMPK*. 7 (4): 242-251. doi: 10.5599/admet.737
14. Chiodi D, Ishihara Y (2024) The role of the methoxy group in approved drugs. *European Journal of Medicinal Chemistry*. 273: 116364. doi: 10.1016/j.ejmech.2024.116364
15. Meena R, Meena P, Kumari A, Sharma N, Fahmi N (2022) Schiff bases and their metal complexes: Synthesis, structure characteristics, and applications. *IntechOpen*. doi: 10.5772/intechopen.108396
16. Arce-Ramos L, Castillo JC, Becerra D (2023) Synthesis and Biological Studies of Benzo[b]furan Derivatives: A Review from 2011 to 2022. *Pharmaceuticals (Basel)*. 16 (9): 1265. doi: 10.3390/ph16091265
17. Nain S, Mathur G, Anthwal T, Sharma S, Paliwal S (2023) Synthesis, Characterization, and Antibacterial Activity of New Isatin Derivatives. *Pharmaceutical Chemistry Journal*. 57: 196-203. doi: 10.1007/s11094-023-02867-4
18. Rajput P, Nahar KS, Rahman KM (2024) Evaluation of antibiotic resistance mechanisms in gram-positive bacteria. *Antibiotics*. 13 (12): 1197. doi: 10.3390/antibiotics13121197

19. Pundir S, Kumar, R, Dinesh R (2016) Role of metal ions in the antimicrobial properties of ligands and their complexes. *Current Medicinal Chemistry*. 23 (13): 1396-1413. doi: 10.2174/092986732604190401100950
20. Khan MZ, Azad AK, Jan S, Safdar M, Bibi S, Majid AMSA, Abdel-Daim MM (2023) An experimental and computational analysis of plant compounds from whole *Urtica dioica* L. plant's essential oil for antioxidant and antibacterial activities. *Metabolites*. 13 (4): 502. doi: 10.3390/metabo13040502
21. Azad AK, Laboni FR, Rashid H, Ferdous S, Rashid SS, Kamal N, Labu ZK, Islam Sarker Z (2020) *In vitro* evaluation of *Cuscuta reflexa* Roxb. for thrombolytic, antioxidant, membrane stabilizing and antimicrobial activities. *Natural Product Research*. 34 (16): 2394-2397. doi: 10.1080/14786419.2018.1538216
22. Azarbanani F, Hadi F, Jafari S, Murthy HA, Azad AK (2023) Antimicrobial, antifungal and antiradical activities of the essential oils from the flower and leaf extracts of Iranian *Ferulago macrocarpa* plant. *Journal of Herbal Medicine*. 39: 100658. doi: 10.1016/j.hermed.2023.100658
23. Hassan AS, Askar AA, Nossier ES, Naglah AM, Moustafa GO, Al-Omar MA (2019) Antibacterial evaluation, in silico characters and molecular docking of Schiff bases derived from 5-aminopyrazoles. *Molecules*. 24 (17): 3130. doi: 10.3390/molecules24173130
24. Iacopetta D, Ceramella J, Catalano A, Mariconda A, Giuzio F, Saturnino C, Sinicropi MS (2023) Metal complexes with Schiff bases as antimicrobials and catalysts. *Inorganics*. 11 (8): 320. doi: 10.3390/inorganics11080320
25. Meng XY, Zhang HX, Mezei M, Cui M (2011) Molecular docking: A powerful approach for structure-based drug design. *Current Computer-Aided Drug Design*. 7 (2): 146-157. doi: 10.2174/157340911795677602
26. Khan A, Hussain S, Ahmad S, Suleman M, Bukhari I, Khan T, Wei DQ (2022) Computational modelling of potentially emerging SARS-CoV-2 spike protein RBDs mutations with higher binding affinity towards ACE2: A structural modelling study. *Computers in Biology and Medicine*. 141: 105163. doi: 10.1016/j.compbimed.2021.105163
27. Agu PC, Afiukwa CA, Orji OU, Ezech EM, Ofoke IH, Ogbu CO, Ugwuja EI, Aja PM (2023) Molecular docking as a tool for the discovery of molecular targets of nutraceuticals in diseases management. *Scientific Reports*. 13 (1): 13398. doi: 10.1038/s41598-023-40160-2
28. Podolski-Renić A, Gašparović AČ, Valente A, Lopez O, Nunes JHB, Kowol CR, Filipović NR (2024) Schiff bases and their metal complexes to target and overcome (multidrug) resistance in cancer. *European Journal of Medicinal Chemistry*. 270: 116363. doi: 10.1016/j.ejmech.2024.116363
29. Yokel RA (2006) Blood-brain barrier flux of aluminum, manganese, iron and other metals suspected to contribute to metal-induced neurodegeneration. *Journal of Alzheimer's Disease*. 10 (2-3): 223-253. doi: 10.3233/jad-2006-102-309
30. Kumar A, Ahmed S, Bhardwaj M, Imtiaz S, Kumar D, Bhat AR, Sood B, Maji S (2024) In vitro anti-microbial, DNA-binding, in silico pharmacokinetics and molecular docking studies of Schiff-based Cu (II), Zn (II) and Pd (II) complexes. *Journal of Molecular Structure*. 1315: 138695. doi: 10.1016/j.molstruc.2024.138695
31. Jorge J, Del Pino Santos KF, Timóteo F, Vasconcelos RRP, Ayala Cáceres OI, Granja IJA, de Souza DM, Frizon TEA, Di Vaccari Botteselle G, Braga AL, Saba S, Rashid HU, Rafique J (2024) Recent advances on the antimicrobial activities of Schiff bases and their metal complexes: An updated overview. *Current Medicinal Chemistry*. 31 (17): 2330-2344. doi: 10.2174/0929867330666230224092830
32. Miners JO, Birkett DJ (1998) Cytochrome P4502C9: an enzyme of major importance in human drug metabolism. *British Journal of Clinical Pharmacology*. 45 (6): 525-538. doi: 10.1046/j.1365-2125.1998.00721.x

Author contribution: MKH & AKZ conceived and designed the study. FH & FSA collected the data. NH & FSA performed data analysis tools. FH, AR, MKS, MNAR, KAAA & AKZ performed the analysis/interpretation of data. FH AKA, RBS & AKZ drafted the manuscript/revising it for important intellectual context. All the authors approved the final version of the manuscript and agreed to be accountable for its contents.

Conflict of interest: The authors declare the absence of any commercial or financial relationships that could be construed as a potential conflict of interest.

Ethical issues: Including plagiarism, informed consent, data fabrication or falsification, and double publication or submission were completely observed by the authors.

Data availability statement: The raw data that support the findings of this article are available from the corresponding author upon reasonable request.

Author declarations: The authors confirm that all relevant ethical guidelines have been followed and any necessary IRB and/or ethics committee approvals have been obtained.